CHEMISTRY
A EUROPEAN JOURNAL

DOI: 10.1002/chem.200701235

On the Conjugation Length for Oligo(ethynylnaphthalene)-Based Molecular Rods

Andrew C. Benniston,* Anthony Harriman,* Dorota B. Rewinska, Songjie Yang, and Yong-Gang Zhi[a]

Abstract: The synthesis is described for a small series of oligomers built from (2, 3, 4 or 6) ethynyl-naphthalene repeat units and end-capped with solubilising 1,2,3-tris-dodecyloxy-benzene groups. These compounds absorb in the near-UV region and exhibit strong fluorescence in both fluid solution and a glassy matrix at 77 K. The spectral profiles are fully consistent with a structurally heterogeneous ground state becoming more planar upon excitation and with the low-temperature glass further stabilising the co-planar orientation. The absorption and fluorescence maxima move towards lower energy with increasing number of repeat units and there is a corresponding increase in the Huang–Rhys factor for the radiative process. The non-radiative rate constants also depend on molecular length and are well explained in terms of the energy-gap law. In contrast, very weak phosphorescence is observed at 77 K for which the peak maximum and lifetime remain insensitive to the number of naphthalene units. The triplet lifetimes recorded at ambient temperature are also independent of the molecular length but the triplet–triplet absorption spectra change throughout the series. These results are discussed in terms of the degree of electronic coupling between adjacent repeat units for each of the relevant excited states. During these studies it was noted that the rate of intersystem crossing to the triplet manifold is but weakly affected by heavy-atom perturbers. A non-fluorescent complex is formed between iodoethane and the molecular rod but the corresponding bimolecular process occurs at well below the diffusion-controlled limit. This behaviour is considered in terms of spin-orbit coupling between the excited states and takes account of the differing conjugation lengths.

Keywords: conducting polymer · energy gap law · fluorescence · naphthalene · photophysics · triplet state

Introduction

Acquiring a deeper understanding of how electronic charge, in the form of either electrons or positive holes, migrates along conjugated organic molecules is of fundamental importance, and indeed such charge-transfer processes have been subjected to innumerable experimental and theoretical studies over the past few decades.[1–6] The level of underlying electron-transfer theory has now advanced to the point at which most aspects of long-range charge migration can be explained. More recently, attention has focussed on the study of medium-length, wire-like supermolecules and oligomeric structures capable of supporting charge transport along the molecular axis.[7–9] Current interest in such highly conjugated, one-dimensional organic wires[10] stems from their potential applications in many diverse areas of materials science, including light-emitting diodes,[11] single-molecule conductors,[12] flash memory devices,[13] chemical sensors,[14] light-harvesting arrays[15] and molecular rectifiers.[16] Closely related research has been directed towards the construction of molecular photonic devices based on highly conjugated organic substrates bridging photoactive terminals.[17,18] The most popular organic modules for building into conductive wires are simple aromatic units such a thiophene,[19] phenylene,[20] biphenylene,[21] fluorene[22] and anthracene.[23] In many cases, the aryl groups are connected through vinyl or acetylene spacer groups that themselves help to modify and control the electronic properties. Although the field has grown rapidly over recent years, only sparse attention has been given to naphthalene-based wires, despite the favourable photophysical properties of such derivatives relative to their smaller counterparts.[24] We report

[a] Dr. A. C. Benniston, Prof. A. Harriman, D. B. Rewinska, Dr. S. Yang, Dr. Y.-G. Zhi
Molecular Photonics Laboratory
School of Natural Sciences, Newcastle University
Newcastle upon Tyne, NE1 7RU (UK)
Fax: (+44) 191-222-6929
E-mail: a.c.benniston@ncl.ac.uk
anthony.harriman@ncl.ac.uk

here on the synthesis and photophysical examination of a small series of ethynylnaphthalene-based molecular-scale wires, with particular focus on their putative role in photonic devices.

It was shown previously that ethynylnaphthalene residues were especially effective bridges for electron exchange between terminal transition metal complexes.[25] A key feature of such systems relates to the relative positioning of excited states localized on the donor, bridge and acceptor units.[24] According to super-exchange theory,[26] the triplet energy of the bridge must be positioned well above those of both donor and acceptor such that the bridge triplet is involved only as a virtual intermediate. In contrast, a hopping mechanism demands that the triplet energy of the bridge lies between those of donor and acceptor.[27] That the triplet energy of a single ethynylnaphthalene unit lies close to that of the donor, but well above that of the acceptor, has been demonstrated[24] but it is quite unknown how this energy will evolve with incremental numbers of added ethynylnaphthalene units. This is critical information for the design of next-generation molecular-scale bridges based on electron exchange and we have sought to explore the systematic evolution of the excited-state properties as a function of molecular length. For this purpose, we have synthesized a series of linear molecular rods containing 2, 3, 4 or 6 ethynylnaphthalene residues capped with solubilising terminal groups (Scheme 1). The longest such system stretches some 50 Å end-to-end and represents a useful model for the bridges envisioned in future photoactive devices.[28]

Apart from establishing the triplet energies of these materials it is also necessary to enquire into the mechanism and efficacy of triplet formation. An important feature of many conducting polymers is that the triplet state seems to be highly localised on a small number of repeat units whereas the corresponding singlet excited state is more extensively delocalised.[29] This behaviour is evident from the disparate delocalisation lengths extracted from spectral curve fitting routines. In turn, this realisation raises concerns about the exact nature of the intersystem-crossing process and also about the delocalisation length of higher-lying triplet states. These upper-lying triplets might become involved as reactive intermediates in certain cases.[30] To explore the triplet manifold we have used the external heavy atom effect[31] in order to perturb the inherent intersystem crossing rates; this feature is also considered to be a viable model for the electron-exchange reactions carried out with ruthenium(II) and osmium(II) poly(pyridine) complexes. It will be shown that this effect is extremely inefficient for this series of compounds, despite the fact that triplet formation takes place under ambient conditions.

Results and Discussion

Synthetic procedure: Preparation of the molecular rods (Scheme 1) followed standard Sonogashira cross-coupling reactions and deprotection procedures.[32] The 1,2,3-trisdodecyloxybenzene moiety was chosen as the terminal unit in an effort to help raise the solubility and to aid in purification of

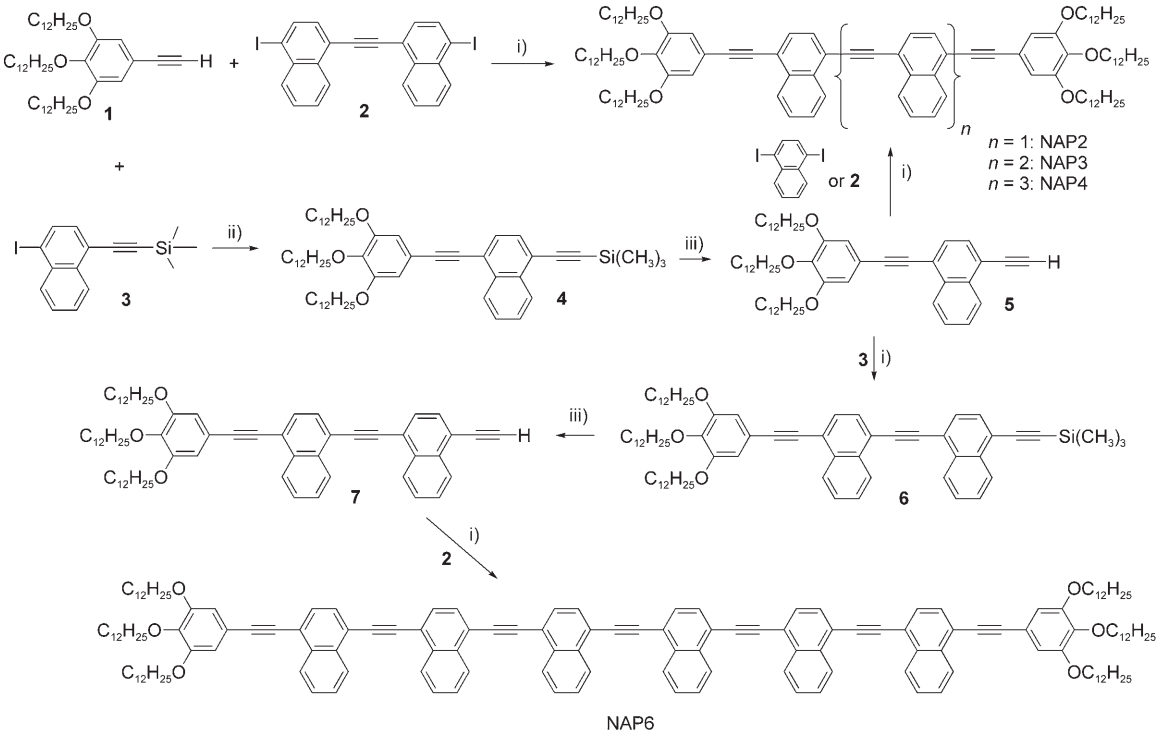

Scheme 1. i) $[Pd(PPh_3)_4]$, CuI, THF, $(iPr)_2NH$, reflux, 12 h; ii) $[Pd(PPh_3)_2Cl_2]$, CuI, THF, $(iPr)_2NH$, 12 h; iii) THF, TBAF, RT, 12 h.

both precursors and final products. Coupling two equivalents of the readily prepared compound **1** with derivative **2** afforded, after work-up and purification, the dimer NAP2 in a respectable 89% yield. Alternatively, coupling **1** with compound **3** afforded derivative **4** which was readily deprotected to give the valuable precursor **5** in 86% yield (two steps). Oligomers NAP3 and NAP4 were obtained by coupling **5** with either 1,4-diiodonaphthalene or with precursor **2**, respectively. The longest oligomer, NAP6, had to be prepared by first coupling **5** with **3** followed by deprotection to give **7**, which was subsequently coupled to derivative **2**. All attempts to produce higher-order oligomers failed because of the poor solubility and extreme difficulty in purifying the products by column chromatography.

Photophysical examination demands small quantities of absolutely pure material. In order to remove all fluorescent impurities, the molecular rods, NAP(n), were subjected to multiple chromatographic separations on silica gel using petroleum ether/CH_2Cl_2 mixtures. Basic compound identification was carried out by mass spectrometry, elemental analysis and ^{1}H NMR spectroscopy. Depicted in Figure 1 is a typical ^{1}H NMR spectrum recorded for NAP2, which shows the associated signals for the alkyl chains and the aromatic protons, together with their assignments. With addition of each ethynylnaphthalene unit, the regions corresponding to protons d, g, b, c and e, f become increasingly more complicated. However, the clear singlet at about $\delta = 6.8$ ppm for protons a remains diagnostic and its relative integral (1:1 NAP2; 2:3 NAP3; 1:2 NAP4; 1:3 NAP6) with respect to protons d, g confirmed isolation of the required target compound. For spectroscopic measurements, these oligomers were subjected to repeated preparative TLC and were deemed of sufficient purity when fluorescence lifetime measurements were strictly mono-exponential.

It has to be emphasized that purification was a tedious and time-consuming process, involving numerous chromatographic separations. Even allowing for the low concentrations needed for emission spectroscopy, it proved difficult to identify suitable solvents for these compounds. Eventually, it was found that methyltetrahydrofuran (MTHF) was a satisfactory solvent for the entire series and this was used throughout the investigation. Although attempts were made to study the effects of solvent polarity on the photophysical properties of these compounds, this line of enquiry was abandoned because of limited solubility.

Photophysical properties: The lowest-energy absorption transition observed for each of these compounds in MTHF at room temperature appears as a relatively broad band with hints of underlying vibrational fine structure. In each case, there is a higher-lying transition with a maximum at around 280 nm. The lowest-energy transition can be deconstructed into a series of Gaussian-shaped bands of common half-width (fwhm = 1200 cm^{-1}).[33] The best fit requires two sets of overlapping bands, each separated by a spacing of about 1000 cm^{-1}. This spacing corresponds to a medium-frequency skeletal vibronic mode coupled to the absorption process. The broadness of the overall band arises from the close positioning of the two transitions. An example of the absorption profile is given in Figure 2 for NAP2. The maximum of the lowest-energy Gaussian (A_{00}) component is assigned to the Franck-Condon absorption transition and is clearly dependent on the number of naphthalene-based repeat units (Table 1). Indeed, the energy of the derived A_{00} transition decreases smoothly with increasing molecular length. The intensity and position of the lowest-energy absorption band are suggestive of the vertical transition being of $^1L_a \leftarrow A_g$ character.[34]

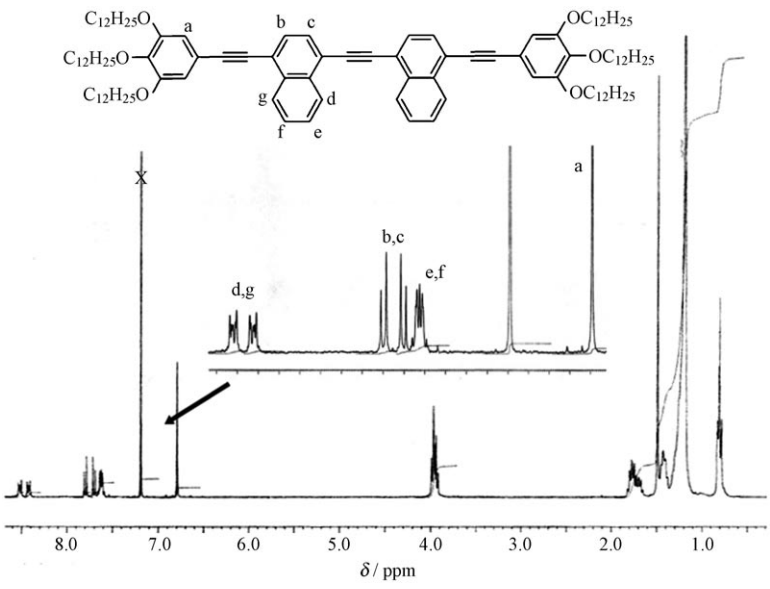

Figure 1. ^{1}H NMR (300 MHz, 25 °C, $CDCl_3$) spectrum for the molecular rod **NAP2** and the aromatic proton assignments. The signal marked X is a residual solvent signal and the water signal is seen at ca. 1.56 ppm.

The various molecular rods display intense fluorescence in deoxygenated MTHF and, as shown in Figure 2 for NAP2, the emission band is relatively narrow and displays vibrational fine structure. There is no obvious indication for mirror symmetry. In each case, the spectral profile remains independent of illumination wavelength and the excitation spectrum shows a good match to the corresponding absorption spectrum over the entire region. The fluorescence spectra could be readily deconstructed into a single series of Gaussian bands, typically four or five such bands of common half-width (fwhm = 1000 cm^{-1}) were needed to fully reconstruct the entire spectrum, each band being separated by

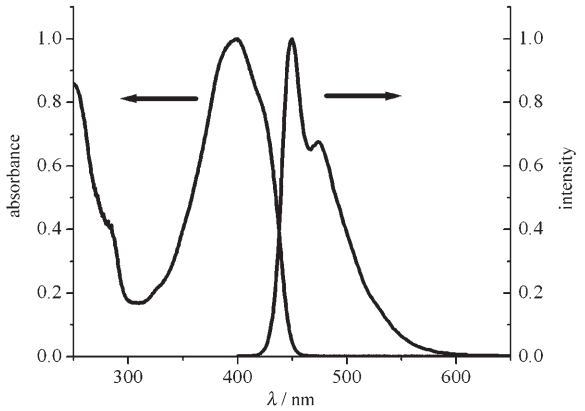

Figure 2. Absorption and fluorescence spectra recorded for **NAP2** in deoxygentated MTHF at 25 °C.

Table 1. Photophysical properties recorded for the singlet-excited states of the various molecular rods in deoxygenated MTHF at room temperature.

Property	NAP2	NAP3	NAP4	NAP6
A_{00} [cm^{-1}]	23367	22498	22129	21859
E_{00} [cm^{-1}]	22222	21459	21008	21859
ϕ_F	0.558	0.526	0.437	0.318
τ_S [ns]	1.1	1.0	0.85	0.70
k_{NR} [10^8 s^{-1}]	4.1	4.7	6.6	9.7
k_{RAD} [10^8 s^{-1}]	5.1	5.3	5.2	4.5
$h\omega_M$ [cm^{-1}]	1095	1180	1280	1120
SS [cm^{-1}][a]	1090	1060	1125	1255
S[b]	0.45	0.53	0.59	0.63

[a] Stokes' shift. [b] Huang-Rhys factor.

an average spacing of 800 cm^{-1}. This spacing corresponds to a relatively low-energy skeletal bending mode ($h\omega_M$) and is clearly much smaller than that extracted from fitting the absorption spectra. The highest-energy Gaussian band (E_{00}), attributed to the 0–0 electronic transition, decreases smoothly with increasing number of repeat units but is always significantly lower than the energy of the corresponding absorption transition (Table 1). The Stokes' shifts (SS), calculated as the minimum energy gap between the deconstructed absorption and emission bands, are quite large and increase progressively with increasing number of repeat units in the molecular backbone (Table 1).

These large Stokes' shifts, taken together with the nature of the absorption/fluorescence profiles, indicate a reasonably large geometry change upon excitation. The structured emission and featureless absorption profiles are fully consistent with a non-planar ground state evolving into a more planar excited singlet state.[35] This behaviour is somewhat analogous to that found for quaterphenyl[36] where the central dihedral angle is reduced upon promotion to the first-excited singlet state. On cooling rapidly to 77 K, the fluorescence spectra undergo a red shift of about 800 cm^{-1}, while the half-widths are decreased by about 20%. This situation can be explained in terms of the frozen glass favouring formation of the fully planar geometry for the excited-singlet state. For the glassy matrix, spectral curve fitting shows that a low-frequency vibrational mode of about 300 cm^{-1} is coupled to decay of the excited state, this being in addition to the medium-frequency mode of about 800 cm^{-1}. The low-frequency vibration is most probably connected with a solvent libration.[37]

$$I_{0,n} = \frac{s^{-S}S^n}{n!} \quad (1)$$

Although there are marked similarities between the emission spectra recorded for the various members of this series, it is clear that there are subtle differences in addition to the red shift. In particular, the ratio of the intensities of the first two vibronic bands depends on the number of repeat units and this is indicative of a change in the Huang–Rhys factor (S).[38] Crude estimates for S were first determined from Equation (1) where $I_{0,n}$ refers to the integrated fluorescence area for the transition from the zero vibrational level in S_1 to the nth vibronic level in S_0.[39] These S values were then used in conjunction with the other parameters derived from emission spectral curve fitting to reconstitute the entire fluorescence according to Equation (2).[30]

$$I(\nu) = \sum_{n=0}^{7} \left\{ \left(\frac{E_{00} - nh\omega}{E_{00}} \right)^3 \frac{S^n}{n!} \exp\left[-4\ln 2 \left(\frac{\nu - E_{00} + nh\omega}{\Delta\nu_{1/2}} \right)^2 \right] \right\} \quad (2)$$

Here, $I(\nu)$ is the normalised fluorescence intensity at wavenumber ν and $h\omega_M$, E_{00} and S are as defined above. The term $\Delta\nu_{1/2}$ refers to the inhomogeneously broadened band half width and the index n indicates the vibrational quantum number. The maximum value of n was restricted to 7; higher values had no effect on the quality of the fit. This spectral analysis was used to refine the value of S (Table 1). It is seen that S increases systematically with increasing number of repeat units, changing from 0.45 for NAP2 to 0.62 for NAP6.

The fluorescence quantum yields (Φ_F) measured in deoxygenated MTHF at room temperature are relatively high but decrease notably with increasing number of repeat units (Table 1). The corresponding excited-singlet state lifetimes (τ_S), obtained from the single exponential decay profiles, are short but also decrease progressively as the molecular length increases (Table 1). The radiative rate constants ($k_{RAD} = \Phi_F/\tau_S$) vary only slightly across the series, in line with the modest changes in the mean emission energy. As such, the transition dipole must remain independent of the number of repeat units. In contrast, the non-radiative rate constants ($k_{NR} = (1/\tau_S) - k_{RAD}$) increase significantly with increasing number of naphthalene units (Table 1).

No phosphorescence could be detected for these compounds in glassy MTHF at 77 K, even after addition of 10% (v/v) iodoethane. Using an optical chopper to remove residual fluorescence, it was possible to observe extremely weak phosphorescence from a snow formed from iodoethane (80%) and MTHF (20%) at 77 K. It was necessary to

employ signal averaging techniques in order to properly resolve this triplet emission (Figure 3). Nonetheless, the phosphorescence signal was found to decay via first-order

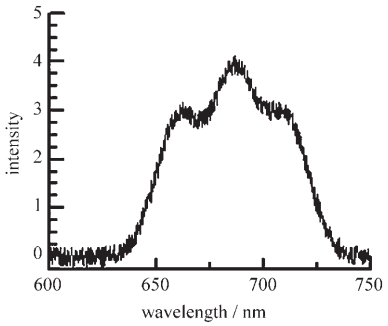

Figure 3. Phosphorescence spectrum recorded for **NAP2** in a deoxygenated 1:4 mixture of MTHF and iodoethane at 77 K.

kinetics with an averaged lifetime (τ_P) of 6 ± 2 ms under these conditions. This lifetime was insensitive to the number of repeat units (Table 2). Likewise, the phosphorescence spectra remained very similar across the series and, in particular, the 0,0 band (λ_{PHOS}) was fairly constant at 670 nm (Table 2). This would suggest that the triplet energy (T_{00}) remains fixed at around 1.85 ± 0.05 eV throughout this series of compounds.

Table 2. Photophysical properties recorded for the triplet-excited states of the various molecular rods in deoxygenated MTHF.

Property	NAP2	NAP3	NAP4	NAP6
λ_{PHOS} [nm]	660	670	665	670
ET [eV][a]	1.88	1.85	1.86	1.85
τ_P [μs][b]	5.1	7.2	5.3	6.5
τ_T [μs]	1.7	1.3	1.3	1.6
λ_{TT1} [nm][c]	470	470	460	490
λ_{TT2} [nm][d]	660	710	720	760

[a] Triplet energy determined from low temperature phosphorescence in 4:1 iodoethane/MTHF. [b] Phosphorescence lifetime recorded at 77 K. [c] High-energy peak in the transient absorption spectrum observed by laser flash photolysis. [d] Low energy peak seen in the transient absorption spectrum.

Further information about the triplet-excited states was sought by nanosecond laser flash photolysis in deoxygenated MTHF and a typical transient differential absorption spectrum is shown in Figure 4. These spectra were weak and it proved difficult to remove all contamination from residual fluorescence. The transient absorption band possessing a maximum at about 470 nm (λ_{TT1}) is common to all four compounds and decays cleanly to the pre-pulse baseline with kinetics that are exclusively first order. The triplet lifetimes (τ_T) measured in deoxygenated solution lie within the range of 1–2 μs (Table 2), and are significantly shortened in the presence of air. At longer wavelength, a much weaker absorption band can be resolved from the baseline but, in this case, the peak maximum (λ_{TT2}) is sensitive to the nature of

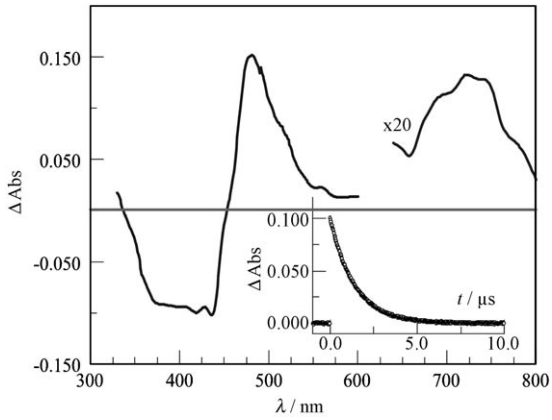

Figure 4. Transient differential absorption spectrum recorded for NAP3 in deoxygenated MTHF following excitation at 355 nm. The insert shows a decay trace recorded at 480 nm.

the compound and moves steadily towards lower energy with increasing number of repeat units (Table 2). This latter band decays with the same lifetime as found for the 470 nm band and both spectral features are formed within the laser pulse.

Effects of increasing molecular length: The most notable spectroscopic changes that accompany an increase in the number of repeat units relate to the absorption and fluorescence spectra (Table 1). There is a progressive decrease in the Franck-Condon absorption maximum (A_{00}) for the first allowed transition and for the corresponding fluorescence process (E_{00}). There is a concomitant increase in the Huang-Rhys factor (S), although other parameters, such as the vibrational spacings and spectral profiles, remain unchanged throughout the series. These effects can be explained within the confines of Figure 5. Here, increasing the molecular

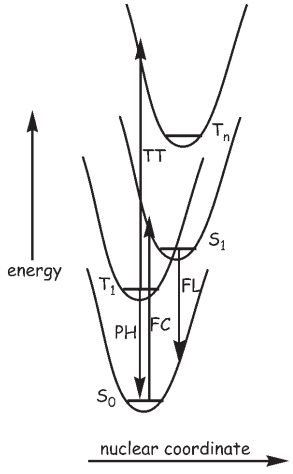

Figure 5. Potential energy diagram showing the main excited states involved in the photophysics of these molecular rods. The processes involved include Franck-Condon excitation (FC), fluorescence (FL), phosphorescence (PH) and triplet–triplet absorption (TT). The Figure implies a large structural change on formation of S_1 and T_n but negligible geometry change between S_0 and T_1.

length leads to a general decrease in the HOMO–LUMO energy gap and, as a consequence, a decrease in A_{00}. This situation demands that the conjugation length increases smoothly with incremental number of naphthalene units, despite the realisation that the ground-state geometry is unlikely to be planar along the molecular axis. Even so, there must be sufficient electron delocalisation for the conjugation length to increase with each added repeat unit. The fluorescence spectral profile is consistent with the excited-singlet state attaining a more planar geometry,[35] such that E_{00} is considerably smaller than A_{00}. Since the Stokes' shift increases steadily with increasing molecular length, it follows that the size of the geometry change accompanying relaxation of the initially formed Franck-Condon state must also increase with each additional naphthalene unit. This geometry change is reflected by S, which increases throughout the series (Table 1).

Indeed, the Huang-Rhys factor can be related to the change in the equilibrium geometries between the ground state and the relaxed singlet-excited state (ΔQ), by way of Equation (3).[40]

$$S = \frac{1}{2}\left(\frac{M\omega_M}{\hbar}\right)\Delta Q^2 \qquad (3)$$

Here, M is the reduced mass of the vibrator and ω_M is the frequency of the coupled vibrational mode. The latter parameter, as extracted from the emission spectral curve fitting routine,[30] remains independent of molecular length so that changes in S can be attributed to variations in ΔQ. Thus, all spectroscopic evidence points to a more substantial change in molecular geometry on illumination as the molecular length increases. Given that the excited-singlet state geometry tends towards planarity, the ground state structure must become more disordered as the molecular length increases. It should be emphasized that the excited-singlet state becomes more planar in a glassy matrix at 77 K. This means that the geometries found under ambient conditions are subject to conformational defects that tend to be eliminated at lower temperature.

We can consider that, for each excited state, the exciton is confined to a characteristic conjugation length set by conformational restrictions and/or electronic factors.[41] Within this model, the energy associated with any particular transition (E_N) is related to the number of repeat units (N) in accordance with Equation (4).[42]

$$E_N = E_M + 2\beta\cos\left(\frac{\pi}{N+1}\right) \qquad (4)$$

Here, E_M is the monomer transition energy and β is the excitation exchange interaction between neighbouring naphthalene units. Given the limited number of compounds, linear plots to Equation (4) were obtained for each of the excited states (Figure 6) and the derived parameters are collected in Table 3. For the Franck-Condon state, believed to possess a rather heterogeneous structure with respect to the mutual alignment of the repeat units, a non-linear, least-squares fit affords values for E_M of 25240 cm^{-1} (396 nm) and $|\beta|$ of 1900 cm^{-1} (0.23 eV). The latter value indicates pronounced electronic coupling between adjacent ethynylnaphthalenes but this is very much less than that observed for poly(*p*-phenylene vinylene) where $|\beta|$ is 8800 cm^{-1} (1.1 eV).[43] A somewhat higher $|\beta|$ (=2000 cm^{-1}) value is found for the relaxed excited-singlet state, where the geometry is more planar, and there is a further increase to $|\beta|$=2400 cm^{-1} in the glassy matrix. This latter environment stabilises the coplanar excited-singlet state. Thus, $|\beta|$ seems to provide a crude estimate of the degree of planarity along the molecular backbone.

A similar $|\beta|$ (=2360 cm^{-1}) is found for the upper-lying triplet state T_{n-1} but a very low $|\beta|$ of about 450 cm^{-1} is derived for the first triplet state T_1 and an intermediate value for the other triplet state T_n (Table 3). As such, we can conclude that adjacent repeat units are but weakly coupled at the T_1 level such that the exciton is essentially confined to a single naphthalene residue. An obvious inference is that the T_1 state possesses a perpendicular geometry that minimizes electronic coupling along the backbone, even at 77 K, but

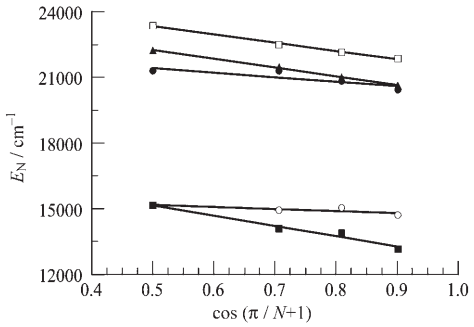

Figure 6. Correlation between the energies of particular transitions and the parameter describing the molecular length, according to Eqn 4. The transitions are: Franck-Condon absorption (□), fluorescence (●), phosphorescence (○), triplet–triplet absorption from T_1 to T_n (▲),and triplet–triplet absorption from T_1 to T_{n-1} (■).

Table 3. Summary of the parameters derived from the length dependence for the optical properties of the various excited states.

State	E_M [cm^{-1}]	$\|\beta\|$ [cm^{-1}]
FC[a]	25240	1900
S_1[b]	24240	2000
S_{77K}[c]	23300	2400
T_1[d]	15615	450
$T_{(n-1)}$[e]	17510	2360
$T_{(n)}$[f]	22465	1040

[a] Franck-Condon state measured by optical absorption. [b] Relaxed singlet excited state measured by fluorescence. [c] Fully relaxed singlet-excited state measured by fluorescence in a glassy matrix at 77 K. [d] First-excited triplet state measured by low temperature phosphorescence. [e] An upper-lying triplet state measured from the low energy peak seen in the transient absorption spectrum. [f] The highest-energy triplet state measured from the high-energy peak in the transient absorption spectrum.

that T_{n-1} adopts a co-planar structure and T_n takes up a structure between these two extremes. This need not be the case, however, since the coupling parameter depends on factors other than the mutual geometry.[44] More reasonably, the atomic orbital coefficients for the carbon atoms connecting naphthalene and ethyne groups are severely reduced for T_1 relative to the other states because of a change in electron distribution or symmetry of the excited state. It should be noted that similar strong confinement of the T_1 triplet exciton has been observed for platinum polyyne derivatives.[45] This finding and ours are somewhat different to those reported for ethylenedioxythiophene oligomers[46] and oligo(9,9-dihexyloligofluorene-2,7-diyl)s,[47] where the triplet energies gradually decrease with an increase in monomer units. We speculate of the possibility that triple bonds help decouple organic units at the triplet level, but further studies are clearly required to see if this is a general phenomenon.

The radiative rate constant (k_{RAD}) remains almost unaffected by changes in molecular length (Table 1) and it is clear that the various excited-singlet states share a common parentage and transition dipole moment. In contrast, the rates of non-radiative decay (k_{NR}) increases with increasing length of the molecular rod (Table 1). This latter effect is easily explained in terms of the Englman–Jortner energy gap law,[48] where k_{NR} is predicted to increase exponentially with increasing S and decreasing E_{00}. The observed rate constants are well described in terms of this model, taking due account of changes in S and E_{00}, but since it is not possible to discriminate between non-radiative decay to form the ground or triplet states, a quantitative fit cannot be attempted. The much smaller energy gap between S_1 and T_1, compared to that involving S_0, could be used to argue in favour of intersystem crossing to the triplet manifold.

Quite remarkably, most of the triplet state properties remain essentially independent of the number of added repeat units in the molecular backbone (Table 2). The triplet energies (E_{TT}), derived from the low temperature phosphorescence spectra remain fairly constant at about 1.86 eV. Consistent with this finding, the triplet decay rates are insensitive to the molecular length, as might be expected on the basis of the Englman–Jortner energy-gap law,[48] at both 77 and 293 K. It follows that the triplet states must share closely comparable S values. Furthermore, the transient differential absorption spectra exhibit a common absorption peak at around 470 nm. This suggests that the energy of the relevant transition, T_1–T_n, is also independent of molecular length. The obvious inference is that, for these two triplet states, the conjugation length is the same throughout the series. Since phosphorescence is measured in a solid matrix at 77 K and triplet–triplet absorption refers to fluid solution at room temperature, it is difficult to attribute this fixed conjugation length to structural distortions. Indeed, for the first-excited singlet state the planar geometry is found at 77 K but a more heterogeneous distribution of geometries abounds at room temperature.

The one exception to this generic triplet-state behaviour concerns the weak transient differential absorption band found in the far-red region. Here, the absorption maximum evolves from 660 nm for NAP2 to 760 nm for NAP6 (Table 2). This latter absorption band corresponds to the T_1–$T_{(n-1)}$ transition and, as such, the energy of the $T_{(n-1)}$ state must decrease with increasing number of repeat units. The spectral evolution is comparable to that found for the S_1 state, thereby raising the possibility that these two states share a common conjugation length that is longer than those of either T_1 or T_n.

Intersystem crossing in the molecular rods: Transient absorption spectroscopy shows that the triplet-excited state is populated in fluid solution at room temperature but that, in each case, the signal is weak. Likewise, phosphorescence was extremely difficult to detect in a glassy matrix at 77 K even in the presence of 10% iodoethane. These findings are consistent with inefficient intersystem crossing to the triplet manifold. Systematic addition of iodoethane to MTHF solutions of each fluorophore shows that extremely high concentrations are needed to effect reasonable levels of fluorescence quenching. Furthermore, in each case, quenching of the steady-state emission exhibits positive deviation from Stern–Volmer kinetics but the singlet-excited state lifetime follows simple Stern–Volmer kinetics (Figure 7), albeit with

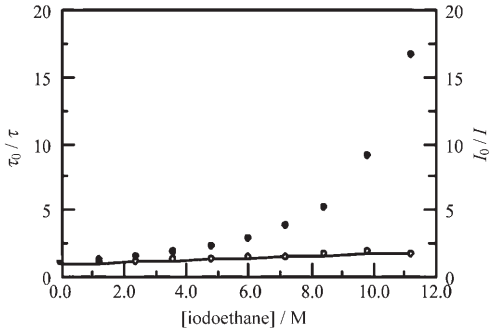

Figure 7. Stern-Volmer plots for the effect of iodoethane on the fluorescence intensity (●) and lifetime (○) of NAP3 in MTHF at room temperature.

an unexpectedly low bimolecular quenching rate constant ($k_Q \approx 2 \pm 1 \times 10^7\,M^{-1}\,s^{-1}$). This behaviour indicates that the heavy-atom quencher forms a weak complex with the molecular-scale rod;[49] the stability constants for formation of the corresponding 1:1 complexes are of the order of $1\,M^{-1}$ and show no obvious correlation with the molecular length. These complexes do not fluoresce with any appreciable efficiency but show enhanced triplet formation. It is also notable that the triplet lifetime is not much shortened by the heavy-atom effect but it is surprisingly short in all cases.

The presence of excess iodoethane has little effect on the absorption spectrum and, in agreement with the limited fluorescence quenching, does not provide significant enhancement of the S_0–T_1 absorption transition. It is generally considered that the external heavy-atom effect promotes spin orbit coupling that is already present in the molecule,

rather than introduces a new process, and that the effect is most notable when the inherent levels of spin orbit coupling are high.[31] That intersystem crossing seems to be ineffective in these molecular-scale rods provides at least partial rationalization for the inability of the heavy-atom effect to promote triplet formation. The nature of the 1:1 complex formed between the organic moiety and iodoethane is mostly likely of charge-transfer origin, although exchange interactions cannot be ruled out, whereby the complex steals intensity from the corresponding singlet-state charge-transfer complex. Spin-orbit coupling of this type is efficient only for states of the same total symmetry and this is clearly not the case for the molecular orbitals involved here. Electron delocalization is greatly reduced for T_1 relative to S_1 and is more in keeping with the ground state. As such, intersystem crossing from T_1 to S_0 is effective, hence the relatively short lifetime for the lowest-energy triplet state, but interconversion from S_1 to T_1 is symmetry forbidden.

Conclusion

In probing the properties of the triplet manifold in these putative molecular-scale rods, two significant factors have emerged. Firstly, the magnitude of electronic coupling between adjacent repeat units at the triplet level depends on the state of excitation. Some triplets, including T_1, are localised onto a small number of repeat units but more extended conjugation is apparent for certain higher-lying triplet states and for the first-excited singlet state. Similar behaviour has been noted previously for other conjugated oligomers but the origin of this property is unclear. Secondly, the compounds are surprisingly resistant to the external heavy-atom effect despite the realisation that intersystem crossing occurs from S_1 to the triplet manifold in the absence of spin orbit perturbation and that the lifetime of the T_1 state is relatively short. It seems likely that these two effects are related and arise as a consequence of changes in the nature of the relevant molecular orbitals. The restricted conjugation length observed for the first triplet state is not due to conformational effects but to poor electronic communication between adjacent naphthalene-based units as imposed by symmetry restrictions. Interestingly, spin orbit coupling is promoted by the internal heavy-atom effect using terminal transition metal complexes where charge-transfer effects are significant. Thus, fluorescence is absent from the closely-related binuclear ruthenium(II) bis(2,2′:6′,2″-terpyridine) complexes and is replaced by fast intersystem crossing to the triplet manifold.[25] The key feature here seems to be the ability to form an intramolecular charge-transfer complex with the perturbing species. Complexation of this type might align the molecular rod in such a way that communication between individual naphthalene residues increases and this might help to circumvent the problems of triplet localization.

Experimental Section

Solvents were dried by standard literature methods before being distilled and stored under nitrogen over 4 Å molecular sieves. ^{1}H and ^{13}C NMR spectra were recorded with a Bruker AVANCE 300 MHz spectrometer. Routine mass spectra and elemental analyses were obtained using in-house facilities. Compounds **1**,[50] **2**[25] and **3**[25] were prepared by literature methods. Even though the final compounds were vacuum dried for several hours, it was not always possible to remove all traces of residual water; this could be seen clearly in the ^{1}H NMR spectra (e.g., Figure 1) at ca. 1.56 ppm. Elemental analyses were also consistent with trace amounts of water impurity. Samples for spectroscopic measurements were subjected to preparative TLC immediately before making the measurement.

Preparation of 4: To a 100 mL two-necked flask were added **1** (2.0 g, 3.1 mmol), **3** (1.09 g, 3.10 mmol), $[Pd(PPh_3)_2Cl_2]$ (150 mg, 0.210 mmol), copper(I) iodide (90 mg, 0.47 mmol) and dry THF (50 mL). The mixture was purged thoroughly with N_2 for one hour before addition of diisopropylamine (15 mL). The solution was refluxed overnight, cooled and the solvent removed under reduced pressure. The crude material was purified by column chromatography on silica gel using petroleum ether/CH_2Cl_2 2:1. Yield 2.37 g, 2.70 mmol, 89%. ^{1}H NMR (300 MHz, 25°C, $CDCl_3$): $\delta = 0.31$ (s, 9H), 0.85 (t, 9H, $J = 6$ Hz), 1.23 (m, 48H), 1.46 (m, 6H), 1.73 (m, 6H), 3.98 (m, 6H), 6.80 (s, 2H), 7.60 (dd (overlapping peaks), 2H, $J = 6$, $J' = 6$ Hz), 7.64 (s, 2H), 8.33 (dd, 1H, $J = 6$, $J' = 6$ Hz), 8.40 ppm (dd, 1H, $J = 6$, $J' = 6$ Hz).

Preparation of 5: To a solution of compound **4** (1.0 g, 1.1 mmol) in dry THF (20 mL) was added TBAF (2 mL, 1 M). The mixture was stirred overnight at room temperature before removing the solvent under reduced pressure. The residue was purified by column chromatography on silica gel using petroleum ether/CH_2Cl_2 2:1. Yield 0.86 g, 1.1 mmol, 97%. ^{1}H NMR (300 MHz, 25°C, $CDCl_3$): $\delta = 0.81$ (t, 9H, $J = 6$ Hz), 1.20 (m, 48H), 1.42 (m, 6H), 1.74 (m, 6H), 3.50 (s, 1H), 3.95 (m, 6H), 6.72 (s, 2H), 7.47 (m, 2H), 7.55 (s, 2H), 8.25 (m, 1H), 8.35 ppm (m, 1H).

Preparation of 6: The procedure described for the preparation of NAP2 was used: **5** (740 mg, 0.920 mmol), **3** (330 mg, 0.940 mmol), $[Pd(PPh_3)_4]$ (32 mg, 0.027 mmol), diisopropylamine (6 mL), THF (60 mL). Yield 830 mg, 0.81 mmol, 88%. ^{1}H NMR (300 MHz, 25°C, $CDCl_3$): $\delta = 0.33$ (s, 9H), 0.80 (t, 9H, $J = 6$ Hz), 1.23 (m, 48H), 1.43 (m, 6H), 1.73 (m, 6H), 3.95 (m, 6H), 6.79 (s, 2H), 7.70 (m, 8H), 8.33 (m, 1H), 8.41 (m, 1H), 8.50 ppm (m, 2H).

Preparation of 7: The procedure described above for the preparation of **5** was used: **6** (830 mg, 0.810 mmol), THF (20 mL), TBAF (3 mL, 1 M). Yield 450 mg, 0.470 mmol, 58%. ^{1}H NMR (300 MHz, 25°C, $CDCl_3$): $\delta =$ 0.80 (t, 9H, $J = 6$ Hz), 1.20 (m, 48H), 1.43 (m, 6H), 1.70 (m, 6H), 3.50 (s, 1H), 3.95 (m, 6H), 6.79 (s, 2H), 7.60 (m, 4H), 7.74 (m, 4H), 8.36 (m, 1H), 8.42 (m, 1H), 8.52 ppm (m, 2H).

General procedure for preparation of final compounds (NAP2): To a 100 mL two-necked flask was added **1** (200 mg, 0.310 mmol), **2** (60 mg, 0.11 mmol), $[Pd(PPh_3)_4]$ (16 mg, 0.014 mmol), copper(I) iodide (6 mg, 0.031 mmol) and dry THF (40 mL). The mixture was purged thoroughly with N_2 for one hour and diisopropylamine (5 mL) added. The solution was refluxed overnight, cooled and the solvents removed under reduced pressure to afford a residue that was purified by column chromatography on silica get using petroleum ether/CH_2Cl_2 2:1. Yield 160 mg, 0.100 mmol, 89%. ^{1}H NMR (300 MHz, 25°C, $CDCl_3$): $\delta = 0.82$ (t, 18H, $J = 6$ Hz), 1.20 (m, 96H), 1.43 (m, 12H), 1.73 (m, 12H), 3.95 (m, 12H), 6.79 (s, 4H), 7.63 (m, 4H), 7.70 (d, 2H, $J = 8$ Hz), 7.80 (d, 2H, $J = 8$ Hz), 8.42 (m, 2H), 8.53 ppm (m, 2H); ^{13}C NMR (75 MHz, 25°C, $CDCl_3$): $\delta =$ 153.36, 139.37, 132.37, 132.28, 129.04, 128.65, 126.40, 126.25, 125.91, 125.74, 121.39, 120.43, 116.67, 110.18, 95.90, 93.24, 85.40, 72.69, 68.69, 30.97, 29.48, 28.77, 28.73, 28.68, 28.47, 28.37, 25.20, 21.68, 13.00 ppm; ES-MS: m/z: calcd for $C_{110}H_{166}O_6$: 1584.49; found: 1584.20 [M^+]; elemental analysis calcd (%) for $C_{110}H_{166}O_6$: C 84.38, H 10.56; found: C 84.15, H 9.87.

NAP3: **5** (165 mg, 0.200 mmol), 1,4-diidonaphthalene (30 mg, 0.079 mmol), $[Pd(PPh_3)_4]$ (12 mg, 0.010 mmol), copper(I) iodide (6 mg, 0.03 mmol), diisopropylamine (6 mL), THF (40 mL). Yield 121 mg,

0.0690 mmol, 88%. ^{1}H NMR (300 MHz, 25°C, $CDCl_3$): $\delta = 0.79$ (t, 18H, $J = 6$ Hz), 1.17 (m, 96H), 1.40 (m, 12H), 1.71 (m, 12H), 3.92 (m, 12H), 6.77 (s, 4H), 7.63 (m, 8H), 7.77 (m, 4H), 8.41 (m, 2H), 8.51 ppm (m, 4H); ^{13}C NMR (75 MHz, 25°C, $CDCl_3$): $\delta = 152.37$, 139.38, 132.34, 132.28, 129.11, 129.06, 128.66, 126.52, 126.44, 125.93, 125.87, 125.74, 121.38, 120.99, 120.36, 116.66, 110.19, 95.95, 93.57, 93.20, 85.41, 72.70, 68.71, 30.96,29.48, 28.77, 28.72, 28.68, 28.59, 28.47, 28.37, 25.20, 21.68, 13.00 ppm; ES-MS: m/z: calcd for $C_{122}H_{172}O_6$: 1734.3; found: 1734.3 [M^+]; elemental analysis calcd (%) for $C_{122}H_{172}O_6 \cdot H_2O$: C 83.60, H 10.01; found C 83.89, H 10.08.

NAP4: **5** (120 mg, 0.150 mmol), **2** (30 mg, 0.057 mmol), [$Pd(PPh_3)_4$] (8 mg, 0.0069 mmol), copper(I) iodide (4 mg, 0.02 mmol), diisopropylamine (5 mL), THF (40 mL). Yield 88 mg, 0.047 mmol, 82%. ^{1}H NMR (300 MHz, 25°C, $CDCl_3$): $\delta = 0.81$ (t, 18H, $J = 6$ Hz), 1.20 (m, 96H), 1.43 (m, 12H), 1.75 (m, 12H), 3.96 (m, 12H), 6.80 (s, 4H), 7.66 (m,10H), 7.84 (m, 6H), 8.44 (m, 2H), 8.57 ppm (m, 6H); ^{13}C NMR (75 MHz, 25°C, $CDCl_3$): $\delta = 152.19$, 139.22, 132.16, 132.10, 128.93, 128.87, 128.47, 126.26, 126.09, 125.68, 125.55, 121.20, 120.89, 120.73, 120.16, 116.46, 110.03, 95.76, 93.43, 93.32, 92.99, 85.21, 72.53, 68.54, 30.77, 29.29, 28.57, 28.53, 28.49, 28.40, 28.28, 28.17, 25.01, 21.48, 18.57, 12.80 ppm; ES-MS: m/z: calcd for $C_{134}H_{178}O_6$: 1888.84; found: 1884.3 [M^+]; elemental analysis calcd (%) for $C_{134}H_{178}O_6 \cdot H_2O$: C 84.58, H 9.53; found: C 84.23, H 9.01.

NAP6: **7** (280 mg, 0.290 mmol), **2** (60 mg, 0.11 mmol), [$Pd(PPh_3)_4$] (20 mg, 0.017 mmol), diisopropylamine (10 mL), THF (50 mL). Yield 144 mg, 0.0660 mmol, 58%. ^{1}H NMR (300 MHz, 25°C, $CDCl_3$): $\delta = 0.81$ (t, 18H, $J = 6$ Hz), 1.20 (m, 96H), 1.43 (m, 12H), 1.78 (m, 12H), 3.98 (m, 12H), 6.80 (s, 4H), 7.71 (m,16H), 7.88 (m, 8H), 8.43 (m, 2H), 8.58 ppm (m, 10H); ES-MS: m/z: calcd for $C_{158}H_{190}O_6$: 2185.2; found: 2185.4 [M^+]; elemental analysis calcd (%) for $C_{158}H_{190}O_6 \cdot 4H_2O$: C 84.07, H 8.84; found: C 84.12, H 9.06.

Methods: Absorption spectra were recorded with a Hitachi U3310 spectrophotometer while all fluorescence studies were made with an Yvon-Jobin fluorolog tau-3 spectrometer. Fluorescence spectra were corrected for spectral imperfections using a standard lamp. Measurements were made using optically dilute solutions after deoxygenation by purging with dried N_2. Fluorescence quantum yields were measured with respect to quinine sulphate ($\Phi_F = 0.58$) in 0.1 M H_2SO_4. Corrected excitation spectra were also recorded under optically dilute conditions. Fluorescence lifetimes were measured by time-correlated, single-photon counting conditions following excitation with a laser diode at 370 nm. After deconvolution of the instrument response function, the temporal resolution of this set-up was ca. 100 ps. Low-temperature studies were carried out with an immersion well Dewar filled with liquid N_2.

Laser flash photolysis studies were made with an Applied Photophysics Ltd LKS.60 instrument. Excitation was made at 355 nm using a frequency-tripled, Nd/YAG laser. The pulse width was ca. 4 ns. A high-intensity, pulsed Xe arc lamp was used for the monitoring beam, kept perpendicular to the excitation beam. The monitoring beam was passed through a high-radiance monochromator and detected with a fast response PMT. Transient differential absorption spectra were recorded point-by-point with five separate records being averaged at each wavelength. Kinetic data were obtained by averaging about 100 individual records collected at a particular wavelength. Solutions for flash photolysis were prepared to possess an absorbance of ca. 0.20 at 355 nm. All solutions were deoxygenated prior to the experiment by purging with dried N_2.

Acknowledgements

This work was supported by EPSRC (GR/S00088/01) and by Newcastle University. The EPSRC-sponsored Mass Spectrometry Service at Swansea is gratefully acknowledged for recording the electro-spray mass spectra.

[1] a) J.-P. Launay, C. Coudret, C. Hortholary, *J. Phys. Chem. B* **2007**, *111*, 6788–6797; b) J. W. Verhoeven, M. N. Paddon-Row, *Int. J. Photoenergy* **2001**, *3*, 79–87.

[2] a) J.-P. Launay, *Chem. Soc. Rev.* **2001**, *30*, 386–397; b) D. M. D'Allesandro, F. R. Keene, *Chem. Soc. Rev.* **2006**, *35*, 424–440; c) A. C. Benniston, A. Harriman, *Chem. Soc. Rev.* **2006**, *35*, 169–179; d) M. N. Paddon-Row, *Aust. J. Chem.* **2003**, *56*, 729–748; e) M. R. Wasielewski, *Chem. Rev.* **1992**, *92*, 435–461; f) J.-L. Brédas, D. Beljonne, V. Coropceanu, J. Cornil, *Chem. Rev.* **2004**, *104*, 4971–5003; g) A. Harriman, R. Ziessel, *Chem. Commun.* **1996**, 1707–1716.

[3] a) D. M. Adams, L. Brus, C. E. D. Chidsey, S. Creager, C. Creutz, C. R. Kagan, P. V. Kamat, S. Lindsay, R. A. Marcus, R. M. Metzger, M. E. Michel-Beyerle, J. R. Miller, M. D. Newton, D. R. Rolison, O. Sankey, K. S. Schanze, J. Yardley, X. Zhu, *J. Phys. Chem. B* **2003**, *107*, 6668–6697; b) S. Skourtis, A. Nitzan, *J. Chem. Phys.* **2003**, *119*, 6271–6276; c) B. P. Paulson, J. R. Miller, W.-X. Gan, G. Closs, *J. Am. Chem. Soc.* **2005**, *127*, 4860–4868; d) A. Van Vooren, V. Lemaur, A. Ye, D. Beljonne, J. Cornil, *ChemPhysChem* **2007**, *8*, 1240–1249; e) V. Coropceanu, J. Cornil, D. A. da Silva Filho, Y. Olivier, R. Silbey, J.-L. Brédas, *Chem. Rev.* **2007**, *107*, 926–952; f) Y. A. Berlin, G. R. Hutchison, P. Rempala, M. A. Ratner, J. Michl, *J. Phys. Chem. A* **2003**, *107*, 3970–3980.

[4] a) A. M. Funston, E. E. Silverman, J. R. Miller, K. S. Schanze, *J. Phys. Chem. B* **2004**, *108*, 1544–1555; b) C. Atienza, N. Martin, M. Wielopolski, N. Haworth, T. Clark, D. M. Guldi, *Chem. Commun.* **2006**, 3202–3204; c) C. Lambert, G. Nöll, J. Schelter, *Nat. Mater.* **2002**, *1*, 69–73; d) F.-R. F. Fan, R. Y. Lai, J. Cornil, Y. Karzazi, J.-L. Brédas, L. Cai, L. Cheng, Y. Yao, D. W. Price, Jr., S. M. Dirk, J. M. Tour, A. J. Bard, *J. Am. Chem. Soc.* **2004**, *126*, 2568–2573; e) W. B. Davis, M. A. Ratner, M. R. Wasielewski, *Chem. Phys.* **2002**, *281*, 333–346; f) C. Joachim, M. A. Ratner, *Nanotechnology* **2004**, *15*, 1065–1075.

[5] a) S. Creager, C. J. Yu, C. Bamdad, S. O'Connor, T. MacLean, E. Lam, Y. Chong, G. T. Olsen, J. Luo, M. Gozin, J. F. Kayyem, *J. Am. Chem. Soc.* **1999**, *121*, 1059–1064; b) L. Groenendaal, M. J. Bruining, E. H. J. Hendrickx, A. Persoons, J. A. J. M. Vekemans, E. E. Havinga, E. W. Meijer, *Chem. Mater.* **1998**, *10*, 226–234; c) M. N. Paddon-Row, S. S. Wong, *Chem. Phys. Lett.* **1990**, *167*, 432–438; d) J. Seth, V. Palaniappan, T. E. Johnson, S. Prathapan, J. S. Lindsey, D. F. Bocian, *J. Am. Chem. Soc.* **1994**, *116*, 10578–10592.

[6] a) J. A. Osaheni, S. A. Jenekhe, J. Perlstein, *J. Phys. Chem.* **1994**, *98*, 12727–12736; b) J. Seth, V. Palaniappan, R. W. Wagner, T. E. Johnson, J. S. Lindsey, D. F. Bocian, *J. Am. Chem. Soc.* **1996**, *118*, 11194–11207.

[7] E. A. Weiss, M. R. Wasielewski, M. A. Ratner, *Top. Curr. Chem.* **2005**, *257*, 103–133.

[8] R. H. Goldsmith, L. E. Sinks, R. F. Kelley, L. J. Betzen, W. Lui, E. A. Weiss, M. A. Ratner, M. R. Wasielewski, *Proc. Natl. Acad. Sci. USA* **2005**, *102*, 3540–3545.

[9] a) J. Wiberg, L. J. Guo, K. Pettersson, D. Nilsson, T. Ljungdahl, J. Mårtensson, B. Albinsson, *J. Am. Chem. Soc.* **2007**, *129*, 155–163; b) M. U. Winters, E. Dahlstedt, H. E. Blades, C. J. Wilson, M. J. Frampton, H. L. Anderson, B. Albinsson, *J. Am. Chem. Soc.* **2007**, *129*, 4291–4297; c) M. P. Eng, T. Ljungdahl, B. Mårtensson, B. Albinsson, *J. Phys. Chem. B* **2006**, *110*, 6483–6491.

[10] a) D. K. James, J. M. Tour, *Top. Curr. Chem.* **2005**, *257*, 33–62; b) P. F. H. Schwab, M. D. Levin, J. Michl, *Chem. Rev.* **1999**, *99*, 1863–1933.

[11] a) V. A. Montes, C. Pérez-Bolívar, N. Agarwal, J. Shinar, P. Anzenbacher Jr, *J. Am. Chem. Soc.* **2006**, *128*, 12436–12438; b) X. Zhang, S. A. Jenekhe, *Macromolecules* **2000**, *33*, 2069–2082; c) X. W. Zhan, Y. Q. Lui, D. B. Zhu, X. Z. Jiang, A. K. Y. Jen, *Synth. Met.* **2001**, *124*, 323–327; d) Y. Liu, H. Ma, A. K. Y. Jen, *J. Mater. Chem.* **2001**, *11*, 1800–1804; e) A. Kraft, A. C. Grimsdale, A. B. Holmes, *Angew. Chem.* **1998**, *110*, 416–443; *Angew. Chem. Int. Ed.* **1998**, *37*, 402–428; f) S.-H. Jung, H. K. Kim, S. H. Kim, Y. H. Kim, S. C. Jeoung, D. Kim, *Macromolecules* **2000**, *33*, 9277–9288.

[12] a) A. Nitzan, *Annu. Rev. Phys. Chem.* **2001**, *52*, 681–750; b) A. Nitzan, M. A. Ratner, *Science* **2003**, *300*, 1384–1389; c) R. L. McCreery, *Chem. Mater.* **2004**, *16*, 4477–4496.

[13] C. Li, W. Fan, B. Lei, D. Zhang, S. Han, T. Tang, X. Liu, Z. Liu, S. Asano, M. Meyyappan, J. Han, C. Zhou, *Appl. Phys. Lett.* **2004**, *84*, 1949–1951.

[14] a) J. Bobacka, A. Ivaska, A. Lewenstam, *Electroanalysis* **2003**, *15*, 366–374; b) J. Sung, R. J. Silbey, *Anal. Chem.* **2005**, *77*, 6169–6173; c) S. W. Thomas, G. D. Joly, T. M. Swager, *Chem. Rev.* **2007**, *107*, 1339–1386; d) F. He, Y. Tang, M. Yu, S. Wang, Y. Li, D. Zhu, *Adv. Funct. Mater.* **2006**, *16*, 91–94.

[15] a) A. Ambroise, C. Kirmaier, R. W. Wagner, R. S. Loewe, D. F. Bocian, D. Holten, J. S. Lindsey, *J. Org. Chem.* **2002**, *67*, 3811–3826; b) N. Nishino, R. W. Wagner, J. S. Lindsey, *J. Org. Chem.* **1996**, *61*, 7534–7544; c) Y. H. Kim, D. H. Jeong, D. Kim, S. C. Jeoung, H. S. Cho, S. K. Kim, N. Aratani, A. Osuka, *J. Am. Chem. Soc.* **2001**, *123*, 76–86; d) T. Sato, D.-L. Jiang, T. Aida, *J. Am. Chem. Soc.* **1999**, *121*, 10658–10659.

[16] R. M. Metzger, *Chem. Rev.* **2003**, *103*, 3803–3834.

[17] a) R. Ziessel, M. Hissler, A. El-Ghayoury, A. Harriman, *Coord. Chem. Rev.* **1998**, *178*, 1251–1298; b) S. Welter, F. Lafolet, E. Ceccetto, F. Vergeer, L. De Cola, *ChemPhysChem* **2005**, *6*, 2417–2427; c) C. Chiorboli, S. Fracasso, M. Ravaglia, F. Scandola, S. Campagna, K. L. Wouters, R. Konduri, F. M. MacDonnell, *Inorg. Chem.* **2005**, *44*, 8368–8378.

[18] a) W. B. Davis, M. A. Ratner, M. R. Wasielewski, *J. Am. Chem. Soc.* **2001**, *123*, 7877–7886; b) J. Wiberg, L. Guo, K. Pettersson, D. Nilsson, T. Ljungdahl, J. Mårtensson, B. Albinsson, *J. Am. Chem. Soc.* **2007**, *129*, 155–163.

[19] a) J. Roncali, *Acc. Chem. Res.* **2000**, *33*, 147–156; b) T. Nakamura, M. Fujitsuka, Y. Araki, O. Ito, J. Ikemoto, Y. Aso, T. Otsubo, *J. Phys. Chem. B* **2004**, *108*, 10700–10710; c) F. Odobel, S. Suresh, E. Blart, Y. Nicolas, J.-P. Quintard, P. Janvier, J-Y. Le Questel, B. Illien, D. Rondeau, P. Richomme, T. Häupl, S. Wallin, L. Hammarström, *Chem. Eur. J.* **2002**, *8*, 3027–3046; d) M. Narutaki, K. Takimiya, T. Otsubo, Y. Harima, H. Zhang, Y. Araki, O. Ito, *J. Org. Chem.* **2006**, *71*, 1761–1768; e) T. Otsubo, Y. Aso, K. Takimiya, *J. Mater. Chem.* **2002**, *12*, 2565–2575; f) J. C. Lacroix, K. I. Chane-Ching, F. Maquére, F. Maurel, *J. Am. Chem. Soc.* **2006**, *128*, 7264–7276; g) L. Trouillet, A. De Nicola, S. Guillerez, *Chem. Mater.* **2000**, *12*, 1611–1621.

[20] a) E. A. Weiss, M. J. Ahrens, L. E. Sinks, A. V. Gusev, M. A. Ratner, M. R. Wasielewski, *J. Am. Chem. Soc.* **2004**, *126*, 5577–5584; b) E. H. A. Beckers, S. C. J. Meskers, A. P. H. J. Schenning, Z. Chen, F. Würthner, R. A. J. Janssen, *J. Phys. Chem. A* **2004**, *108*, 6933–6937; c) A. M. Ramos, E. H. A. Beckers, T. Offermans, S. C. J. Meskers, R. A. J. Janssen, *J. Phys. Chem. A* **2004**, *108*, 8201–8211; d) W. B. Davis, W. A. Svec, M. A. Ratner, M. R. Wasielewski, *Nature* **1998**, *396*, 60–63.

[21] a) A. C. Benniston, A. Harriman, P. Li, C. A. Sams, *J. Am. Chem. Soc.* **2005**, *127*, 2553–2564; b) M. Polson, C. Chiorboli, S. Fracasso, F. Scandola, *Photochem. Photobiol. Sci.* **2007**, *6*, 438–443.

[22] a) R. Gómez, D. Veldman, R. Blanco, C. Seoane, J. L. Segura, R. A. J. Janssen, *Macromolecules* **2007**, *40*, 2760–2772; b) C. Wang, A. S. Batsanov, M. R. Bryce, G. J. Ashwell, B. Urasinska, I. Grace, C. J. Lambert, *Nanotechnology* **2007**, *18*, 044005; c) Y. Chen, M. E. El-Khouly, X.-D. Zhuang, N. He, Y. Araki, Y. Lin, O. Ito, *Chem. Eur. J.* **2007**, *13*, 1709–1714.

[23] a) P. Belser, R. Dux, M. Baak, L. De Cola, V. Balzani, *Angew. Chem.* **1995**, *107*, 634–637; *Angew. Chem. Int. Ed. Engl.* **1995**, *34*, 595–598; b) A. C. Benniston, A. Harriman, D. J. Lawrie, S. A. Rostron, *Tetrahedron Lett.* **2004**, *45*, 2503–2506; c) A. El-Ghayoury, R. Ziessel, *Tetrahedron Lett.* **1997**, *38*, 2471–2474; d) G. Nöll, M. Avola, M. Lynch, J. Daub, *J. Phys. Chem. C* **2007**, *111*, 3197–3204.

[24] A. El-Ghayoury, A. Harriman, R. Ziessel, *J. Phys. Chem. A* **2000**, *104*, 7906–7915.

[25] A. C. Benniston, S. Mitchell, S. A. Rostron, S. Yang, *Tetrahedron Lett.* **2004**, *45*, 7883–7885.

[26] H. M. McConnell, *J. Chem. Phys.* **1961**, *35*, 508–515.

[27] a) A. El-Ghayoury, A. Harriman, A. Khatyr, R. Ziessel, *J. Phys. Chem. B* **2000**, *104*, 1512–1523; b) A. El-Ghayoury, A. Harriman, A. Khatyr, R. Ziessel, *Angew. Chem.* **2000**, *112*, 191–195; *Angew. Chem. Int. Ed.* **2000**, *39*, 185–189.

[28] A. Harriman, A. Khatyr, R. Ziessel, A. C. Benniston, *Angew. Chem.* **2000**, *112*, 4457–4460; *Angew. Chem. Int. Ed.* **2000**, *39*, 4287–4290.

[29] C. Rothe, K. Brunner, I. Bach, S. Heun, A. P. Monkman, *J. Chem. Phys.* **2005**, *122*, 084706.

[30] A. C. Benniston, A. Harriman, P. Li, C. A. Sams, *J. Phys. Chem. A* **2005**, *109*, 2302–2309.

[31] S. P. McGlynn, T. Azumi, M. Kinoshita, *Molecular Spectroscopy of the Triplet State*, Prentice Hall, Englewood Cliffs, NJ, **1969**.

[32] K. Sonogashira, Y. Tohda, N. Higihara, *Tetrahedron Lett.* **1975**, *16*, 4467–4470.

[33] A. Amini, A. Harriman, A. Mayeux, *Phys. Chem. Chem. Phys.* **2004**, *6*, 1157–1164.

[34] J. B. Birks, *Photophysics of Aromatic Molecules* Wiley-Interscience, London, **1970**.

[35] a) I. B. Berlman, *J. Phys. Chem.* **1970**, *74*, 3085–3093; b) I. B. Berlman, H. O. Wirth, O. J. Steingraber, *J. Phys. Chem.* **1971**, *75*, 318–325; c) I. B. Berlman, *J. Phys. Chem.* **1973**, *77*, 562–567.

[36] B. D. Allen, A. C. Benniston, A. Harriman, I. Llarena, C. A. Sams, *J. Phys. Chem. A* **2007**, *111*, 2641–2649.

[37] J. P. Claude, T. J. Meyer, *J. Phys. Chem.* **1995**, *99*, 51–54.

[38] T. W. Hagler, K. Pakbaz, K. F. Voss, A. J. Heeger, *Phys. Rev. B* **1991**, *44*, 8652–8666.

[39] S. P. Kennedy, N. Garro, R. T. Phillips, *Phys. Rev. B* **2001**, *64*, 115206.

[40] T. Markvart, R. Greef, *J. Chem. Phys.* **2004**, *121*, 6401–6405.

[41] a) C. A. M. Borges, A. Marletta, R. M. Faria, F. E. G. Guimaraes, *Brazilian J. Phys.* **2004**, *34*, 590–592; b) M. Wohlgenannt, X. M. Jiang, Z. V. Vardeny, *Phys. Rev. B* **2004**, *69*, 241204; c) J. L. Brédas, D. Beljonne, J. Cornil, D. A. dos Santos, Z. Shuai, D. D. C. Bradley, M. Schott, *Philos. Trans. R. Soc. London* **1997**, *355*, 735–746.

[42] a) R. Chang, J. H. Hsu, W. S. Fann, K. K. Liang, C. H. Chang, M. Hayashi, J. Yu, S. H. Lin, E. C. Chang, K. R. Chuang, S. A. Chen, *Chem. Phys. Lett.* **2000**, *317*, 142–152; b) O. Mirzov, I. G. Scheblykin, *Phys. Chem. Chem. Phys.* **2006**, *8*, 5569–5576.

[43] J. W. Yu, W. S. Fann, F. J. Kao, D. Y. Yang, S. H. Lin, *Synth. Met.* **1994**, *66*, 143–148.

[44] M. Y. Lavrentiev, W. Barford, *J. Chem. Phys.* **1999**, *111*, 11177–11182.

[45] D. Beljonne, H. F. Wittmann, A. Köhler, S. Graham, M. Ypunus, J. Lewis, P. R. Raithby, M. S. Khan, R. H. Friend, J. L. Brédas, *J. Chem. Phys.* **1996**, *105*, 3868–3877.

[46] D. Wasserberg, S. C. J. Meskers, R. A. J. Janssen, E. Mena-Osteritz, P. Bäuerle, *J. Am. Chem. Soc.* **2006**, *128*, 17007–17017.

[47] D. Wasserberg, S. P. Dudek, S. C. J. Meskers, R. A. J. Janssen, *Chem. Phys. Lett.* **2005**, *411*, 273–277.

[48] R. Engleman, J. Jortner, *Mol. Phys.* **1970**, *18*, 145–164.

[49] T. L. Nemzek, W. R. Ware, *J. Chem. Phys.* **1975**, *62*, 477–489.

[50] J. Wu, M. D. Watson, L. Zhang, Z. Wang, K Müllen, *J. Am. Chem. Soc.* **2004**, *126*, 177–186.

Received: August 8, 2007
Published online: October 23, 2007

